

# Design and Analysis of End-of-Arm Tooling of Robot for Industrial Washing Application



<sup>#1</sup>MayurShedge, <sup>#2</sup>PrashantAnerao

<sup>1</sup>mayur.3655@gmail.com

<sup>2</sup>prashant.anerao@gmail.com

<sup>#1</sup>Mechanical Engineering Department, Pune University  
VIIT, Pune

<sup>#2</sup>Penta Designers and Engineers Pune, Maharashtra, India

## ABSTRACT

The automobile industries has long relied on industrial robotic washing system that guaranty the efficient cleaning of identical work pieces. End-of-Arm Tooling (EOAT) is an essential part of an industrial robotic washing system that enables the robot to do a particular task. Previous automation based system found to be relatively inflexible to accommodate variation in work pieces. It also refers to very high cost being used for variety of work pieces. This paper presents the design and analysis of EOAT for accomplishing firm and stable gripping and manipulation of four different types of cylinder heads having different geometrical properties at a time when comes in batch production using change part concept. The proposed EOAT is a gripper comprised of two parallel fingers that can be folded and unfolded by the action of pneumatic actuator. The design of EOAT is obtained through a systematic modeling. This designed EOAT has been analyzed on various factors so that it will not fail or component will not drop down from fingers. The device design is validated through Finite Element Analysis (FEA) model correlation studies. The CAD modeling is carried out on Solidworks tool and FEA analysis is carried out on ANSYS tool. This paper also aims at laying a solid theoretical and technical foundation for general procedure of design of EOAT.

**Keywords**— EOAT design, FEA analysis, Gripping force, Industrial robot washing system, Solidworks.

## ARTICLE INFO

### Article History

Received :18<sup>th</sup> November 2015

Received in revised form :

19<sup>th</sup> November 2015

Accepted : 21<sup>st</sup> November , 2015

**Published online :**

22<sup>nd</sup> November 2015

## I. INTRODUCTION

The automobile industries has long relied on transfer stations that guaranty the efficient and timely processing and cleaning of identical work pieces. When work pieces are less than clean, they will not operate to their fullest. Even the tiniest chip which might be left after the mechanical production process or any trace of oil or dirt would detract from the quality of engines. But in order to clean and process parts effectively, stations required very finely tuned elements that traditionally have been relatively inflexible and difficult to adapt to different parts. To overcome this problem, the new kind of cleaning module has been developed which has been more flexible than older system. The new cleaning module combines cleaning

methods with the flexibility of a fully automatic 6-axis robot integrated into treatment module. The robot is equipped with a newly developed gripper which can be easily adjusted to accommodate different work pieces having irregularly shaped cavities or drill holes with weight up to 70 kg whose design is a primary objective.

**Balkeshwar Singh et al** described robot technology and goes into more depth about robots are used [1][2]. **Samson Khoo Hock Chye et al** presented the design and analysis of robot gripper for 10kg payload [3]. **Burak Doganet al** presented design and development of two fingered gripper and four fingered multipurpose gripper actuated by

pneumatic actuator along with the design of motion control card for control of pneumatic valves [4].

**Yimin Song et al** provides optimal design of 1T3R parallel manipulator on the basis of kinematic analysis. By means of the screw theory and the displacement group theory, they have analyzed the mobility and formulated 4x4 Jacobian matrix [5].

**Qiang Zeng et al** presented the structural design process of Tri-pyramid robot. They have analyzed kinematic position solutions and evaluated workspace with variation of structural parameters [6].

**Z. Dougeri Li et al** showed an asymptotic convergence of the applied force error. They have presented an adaptive position force controller for a robotic finger with a soft hemispherical tip in contact with a rigid surface [7].

**Joong-Jo Park et al** developed the 6-axis force/moment sensor for an intelligent robot's gripper using parallel-plate beams (PPBs) that measure the forces  $F_x$ ,  $F_y$  and  $F_z$  and moments  $M_x$ ,  $M_y$  and  $M_z$  simultaneously [8].

**V.C. Moulianitis et al** presented an approach for the modeling of the evaluation process in the conceptual design phase. They have presented mechatronics index in terms of intelligence, flexibility and complexity of design alternatives [9].

**R. Saravanan et al** proposed use of intelligent techniques like Multi-objective Genetic Algorithm (MOGA), Elitist Non-dominated Sorting Genetic Algorithm (NSGA-II) and Multi-objective Differential Evolution (MODE) to solve the problem [10].

**Mohammed Khadeeruddin et al** presented the design and analysis of jaw actuated pneumatic gripper. The force and torque for the gripper have been calculated for different set of conditions [11].

**Songhui Nie et al** presented a general study of the kinematic configuration analysis of planar mechanisms with R-pairs. They have described an efficient and reliable approach for type identification of Basic Kinematic Chains (BKC) [12]. **Jyh-Jone Lee et al** proposed path synthesis of a gripper-object mechanism with two rolling pairs. They have derived the design equations for kinematic synthesis

[13]. **Dalibor Petkovic et al** in their work designed an adaptive under actuated compliant gripper with distributed passive compliance which can grip objects of any shape. They have used iterative finite element method optimization process along with An Adaptive Neuro-Fuzzy Inference System (ANFIS) to obtain an optimal topology of gripper [14]. **Rim Boughdiri et al** presented a design of a multi fingered robot hand having five fingers with 20 DOF. Numerical and 3D simulation results have been used to prove that model based controller can achieve high positioning accuracy [15]. **Sandeep Krishnan et al** presented a design and development of micro-clasp gripper. The experimental validation confirms that irregularly shaped micro particles can be successfully grasped and repositioned regardless of their initial orientation and position [16]. **Arockia Selvakumar A et al** presented a model of 3 DOF parallel manipulator (Tripod and Tri-Glide) using screw joints for very accurate positioning. Authors have performed the position analysis of same manipulator [17]. **Gualtiero Fantoni et al** presented a methodology for supporting the selection of gripper including information about grasping principles, releasing strategies and problems concerning the automatic assembly. This paper described the basic information regarding the development of an expert system for the selection of robot gripper [18]. **Alaa Hassana et al** presented a design of robot gripper which can be used in pick and place operation in various automation processes. Kinematic model is found and singular configurations are identified [19]. **Yi Lu et al** presented a design of novel 6 DOF 3 UPS parallel manipulator. Kinetostatic analysis of the same manipulator is carried out which is different than normal analysis and jacobian and Hessian matrices are derived [20]. **Nobuaki Nakazawa et al** presented the force control of a robot gripper that is modeled on the basis of human grasping schemes [21]. **Olivier Millet et al** presented the gripper design based on the combination of ground-links and moving pin-joints with the principle of the amplification mechanism. Kinematics characterization of different types of grippers is determined [2

## II. DESIGN OF EOAT

### A. Component Description

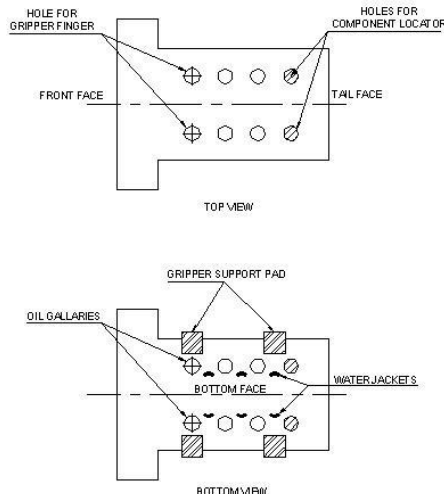


Fig. 1 Gripper and locator positions on component

The component to be washed is an engine cylinder head of gasoline and/or diesel engine having weight upto 70kg. There are two critical areas in engine cylinder head namely oil galleries and water jackets. These areas have to be clean properly and precisely for efficient operations of engine heads. EOAT should be positioned in such way that gripper's top finger and bottom finger support pads should be positioned accurately and precisely at their respective positions.

### A. Types of Grip

The grips are generally of two types namely Friction grip and Encompassing grip.

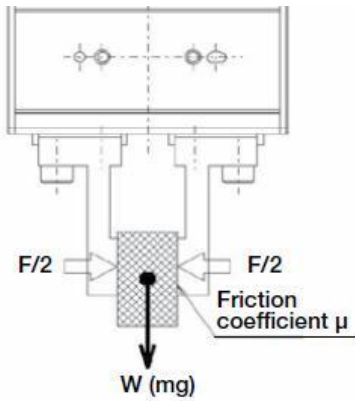


Fig.2 Forces acting on friction grip

Friction grip rely totally on the force of the gripper to hold the part, the “squeeze” of the gripper does all of the work. Stronger inertial forces are applied to a work part by gravity and moments.

$$F = \frac{mg \times 4}{\mu \times n}$$

When the friction coefficient  $\mu$  is between 0.1 and 0.2 with 2 fingers and factor of safety to be consider as 4,

$$F = \frac{mg \times 4}{(0.1 \sim 0.2) \times 2}$$

$$F = (10 \sim 20) \times mg \quad (1)$$

Therefore necessary gripping force for friction grip must be 10 to 20 times the component weight or more.

Encompassing jaws add stability and power by cradling the part. Encompassing jaws provide a major advantage because the jaws must be driven open for a part to be dropped from an encompassing grip. It requires less force to hold the object.

Confirm that the vertical load applied to each finger is the allowable load or less. Calculate moments  $M_a$  and  $M_c$  using  $L_1$  and moment  $M_b$  using  $L_2$ . Confirm that the moment applied to each finger is the maximum allowable load moment or less. Allowable external force when the moment load is applied to each jaw.

$$\text{Allowable load } F \text{ (N)} = \frac{M \text{ (Maximum moment Nm)}}{L \text{ (mm)} \times 10^{-3}}$$

As per Rule of Thumb, The encompassing grip requires one fourth the force required to hold the same object as in case of a friction grip.

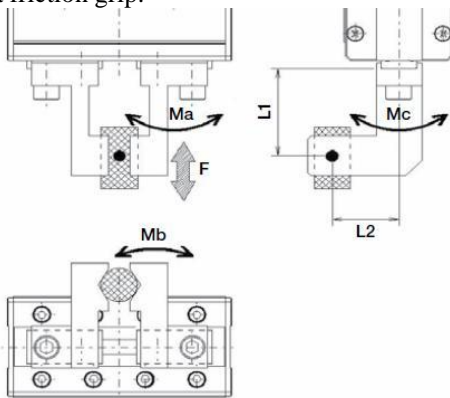
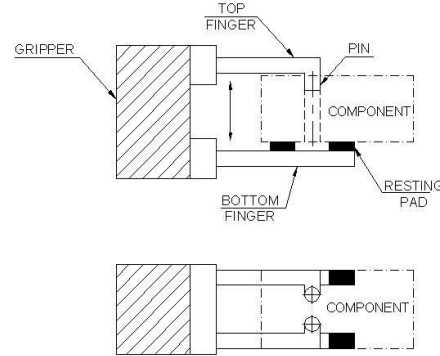


Fig. 3 Forces acting on Encompassing grip

B. Criteria for Stable Gripping

The principle objective of the gripper is to grip the component firmly having weight up to 70 kg so that it will not fall or damage while going through various washing operations like injection fluid (up to 2 bar), specific wash, high pressure wash (up to 60 bar) and compressed air blow. The maximum speed of the robot will be 2 m/s and it is required that total washing cycle should be complete in 109 seconds. Hence gripper should be designed in such way that it will not fail due to robot speed or due to inertia while going through various washing operations. Failure of the gripper leads to failure of total washing machine module.

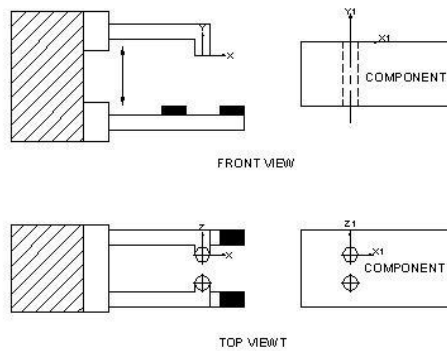


C. Fig. 4 EOAT with component

EOAT consists of a pneumatic gripper having definite stroke of 150mm. Stroke of the gripper can be adjusted as per the component size. There are top and bottom fingers for gripping purpose which can be folded and unfolded. Top fingers have two pins which will get inserted into respective holes on component. This will lead to the encompassing grip which will cradle the part. Lower finger have two support pads which are located exactly opposite to the pins. The EOAT has been designed in such way that being self-centring gripper, force exerted by the top finger pin will be balanced by two resting pads on bottom finger as shown in Fig. 4. This will give stable gripping.

D. EOAT Concept Generation to Obtain Rated Flexibility

(2) For proper and precise gripping of component, XYZ axes of component should exactly match with XYZ axes of gripper as shown in Fig. 5. Component should be picked up by the robot in such a way that top finger pins should be inserted in desired holes and bottom finger resting pads must be placed on opposite side of inserting pins. This should be carried out repeatedly. Proper gripping of component is also ensured by subassemblies like Poke yoka plate, component aligner unit, Singling unit and lifting table. If it is does not match exactly then either component may fall from gripper or it may leads to wrong gripping.



E. Fig. 5 EOAT concept

As system is used for four different types of components at a time, by adjusting the stroke of the pneumatic cylinder different types of components can be handles. Hence required flexibility can be achieved and no need to change gripper for each type of component. For each of the component, stroke will be changed as per the locations of the holes on component for insertion of pins. As shown in Fig. 6, Let maximum stroke of gripper be (a+b). Suppose for the component 1, distance a, b and (a+b) can be adjusted by photo sensors arrangement which is located on entry side conveyor. These sensors gives input to the gripper sensors regarding which component is to be grip and accordingly stroke of the gripper is adjusted to accommodate required component. Stroke of the gripper will be adjusted equally on both sides of the zero line as shown in Fig. 6.

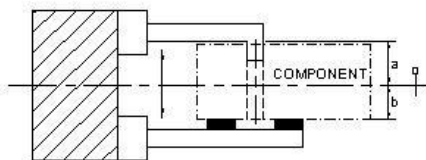


Fig. 6 Flexibility of EOAT

F. Gripper Orientations With Object

When gripper with encompassing grip along with firmly held component is moving in working space, its orientations and forces acting on it are shown in Fig. 7. As shown in (a) When gripper is moving vertically along Z axis, moment  $M_x$  is acting on gripper. Moment  $M_x$  should be less than allowable moment. There is no prominent effect of frictional force  $F_r$  on gripper finger when moving in upward or downward direction but due to component weight  $M_g$  and tooling length  $L$ , moment of  $(M_g \times L)$  will act on gripper finger. When gripper is moving horizontally along X axis, frictional force  $F_r$  will try to drag out the component from finger. This may lead to drop down or failure of EOAT. To avoid this failure, gripping force should be sufficiently large to overcome frictional force  $F_r$ .

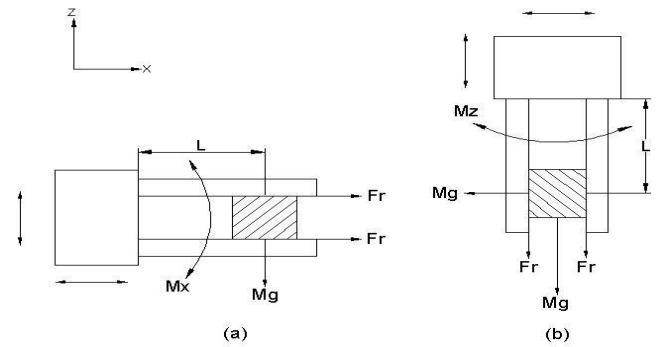


Fig. 7 Orientations of gripper with object

Another gripping position as shown in (b). When gripper is moving horizontally along X axis, moment  $M_z$  is acting on gripper. Value of this moment  $M_z$  should be less than allowable moment. Component weight  $M_g$  and tooling length  $L$  will exert a moment of  $(M_g \times L)$  on gripper finger. When gripper is moving vertically along Z axis, frictional force  $F_r$  along with component weight  $M_g$  will try to push out the component from finger. gripping force should be sufficiently large to overcome a force caused due to frictional force  $F_r$  and component weight  $M_g$ .

G. Orientations and Part Shape

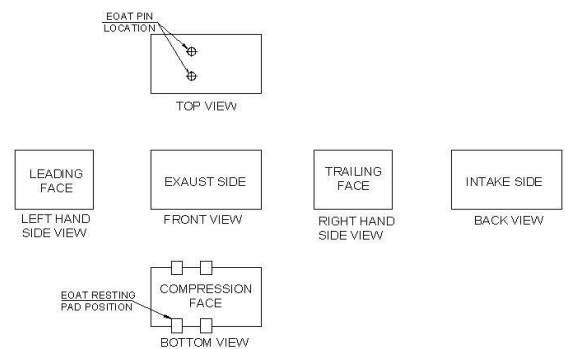


Fig. 8 Component orientations

Component orientations are as shown in Fig. 8. Flow of component on entry side and exit side conveyor is from left to right in batch production. Component is resting on compression face with front side leading. Resting pads are positioned on compression face or block contact face and top finger pins are located on opposite side face of compression face. Weight of the components to be handled is up to 60kg.

H. Environmental Conditions

Being washing operations, working conditions will be wet and humid. Operating temperature will be in the range of  $-28^\circ$  to  $+82^\circ$ , operating pressure will be 4 bar (2 bar to 8 bar).

I. Tooling Length

Tooling length is the distance between jaw surface and grip point. Jaw tooling should be designed so that the grip point is as close to the jaw surface as possible. As the grip point is moved away from the jaw surface, the applied

moment causes jaw friction to increase, resulting in reduced effective grip force.

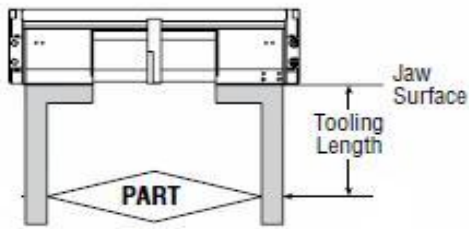


Fig. 9 Tooling length

J. Gripper



Fig.10 Pneumatic gripper, (PHD, USA)

Gripper is selected based on type of application, working conditions, component weight, size, shape and speed of the robot. Selected gripper is of PHD, USA make. (US Patent #7,490,881) designated as GRR 1 2 – 6 – 63 x 150 - Z1 - H47

K. Grip Force

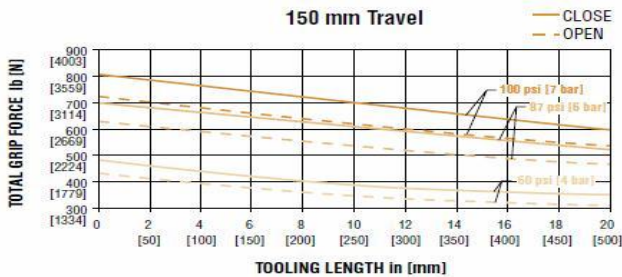


Fig. 11 Total grip force Vs Tooling length (PHD, USA)

Grip force per jaw equals half of the total grip force. Grip force selected from Fig. 11 with tooling length of 350 mm and operating pressure of 4 bar is 1770 N. Tooling length factor of 0.79 is selected.

Maximum allowable forces and moments are obtained from gripper catalogue as

$$F_a = 15570 \text{ N}$$

$$M_x = 880 \text{ Nm}$$

$$M_y = 715 \text{ Nm}$$

$$M_z = 715 \text{ Nm}$$

(3)

As system is employed to washing environment with wet surrounding, material selected is AISI 309S.

L. Jaw Cross-Section Selection

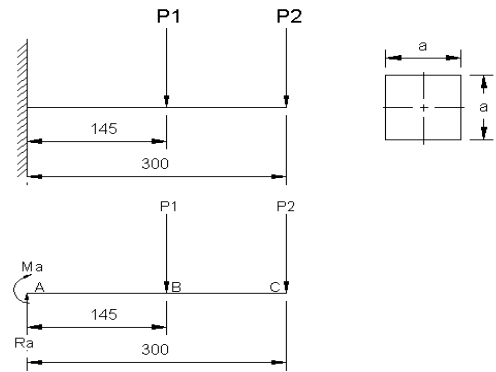


Fig. 12 Jaw cross-section and free body diagram  
Length (L) = 300 mm (4)

Factor of safety (FOS) = 2

Component weight (Wc) = 70 kg = 686.7 N

Total gripping force (Gf) = 1770 N

Total force acting on finger (Wt) = Wc + Gf = 2456.7 N (5)

Number of fingers (N) = 2

$$F_{P1} = F_{P2} = \frac{W_t}{4} = 614.18 \text{ N} \quad (6)$$

$$\text{Support reaction at A (Ra)} = P1 + P2 = 1228.36 \text{ N} \quad (7)$$

Moment at point A,

$$M_a = (P1 \times 145) + (P2 \times 300) = 273310.1 \text{ N-mm} \quad (8)$$

**Shear Force Diagram:**

$$\text{Shear force between (B-C)} = -614.18 \quad (9)$$

$$\text{Shear force between (A-B)} = -(614.18 + 614.18) = -1228.36 \text{ N}$$

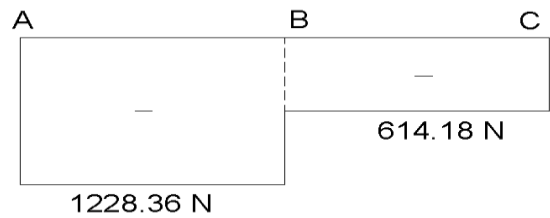


Fig. 13 Shear Force Diagram

**Bending Moment Diagram:**

Bending Moment at point C = 0

$$\text{Bending Moment at B} = -(614.18 \times 155) = 95197.9 \text{ N-mm}$$

$$\text{Bending Moment at A} = -[(614.18 \times 145) + (614.18 \times 300)] = -273310.1 \text{ N-mm} \quad (10)$$

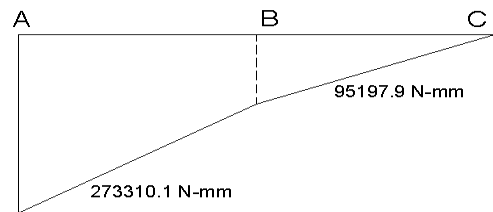


Fig. 14 Bending Moment Diagram

As FOS = 2,

$$\text{Working Stress } (\sigma) = \frac{\text{Critical Stress}}{\text{FOS}} = 102.5 \text{ MPa} \quad (11)$$

$$\text{Moment of inertia (I)} = \frac{a^4}{12} \quad (12)$$

$$\text{Section modulus (Z)} = \frac{I}{y}; \text{ As } y = \frac{a}{2}, Z = \frac{a^3}{6} \quad (13)$$

$$\text{Working stress } (\sigma) = \frac{M}{Z} = \frac{(\text{Max. Bending Moment} \times 6)}{a^3} \quad (14)$$

This gives,  $a = 25.19 \text{ mm}$

Taking into consideration 5 million cycles of operations, selecting next cross-section size which is 32 mm.

Hence selected cross-section,  $a = 32 \text{ mm}$ .

**M. Stress Analysis of Fingers**

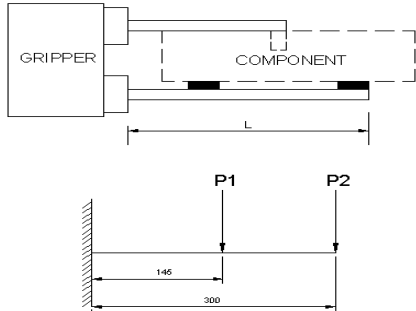


Fig. 15 EOAT block diagram

**Stress Analysis of Bottom Finger:**

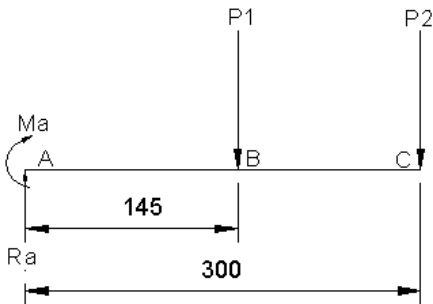


Fig. 16 Free body diagram of bottom finger

Total force acting on fingers,

$$W_t = [(\text{Component weight} + \text{Finger weight}) \times 9.81] + \text{Gripping force} = 2626.51 \text{ N} \quad (15)$$

Number of fingers (N) = 2

$$\text{Load on each finger } (P) = \frac{W_t}{N} = 1313.25 \text{ N} \quad (16)$$

$$\text{Therefore, } P_1 = P_2 = \frac{P}{4} = \frac{1313.25}{4} = 328.31 \text{ N}$$

$$\text{Support reaction at A, } R_a = P_1 + P_2 = 656.62 \text{ N} \quad (17)$$

Moment at A,

$$M_a = (P_1 \times 145) + (P_2 \times 300) = 146097.95 \text{ N-mm} \quad (18)$$

**Shear Force Diagram:**

Shear force between (B-C) = - 328.31

Shear force between (A-B) = - (328.31 + 328.31) = - 656.62 N

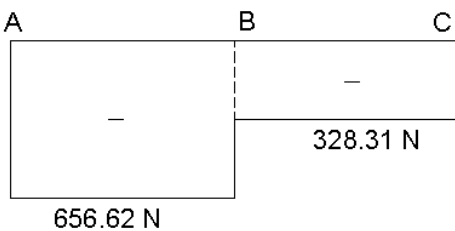


Fig. 17 Shear force diagram of bottom finger

**Bending Moment Diagram:**

Bending Moment at point C = 0

Bending Moment at B = - (328.31 x 155) = 50888.05 N-mm

$$\text{Bending Moment at A} = - [(328.31 \times 145) + (328.31 \times 300)] = - 146097.95 \text{ N-mm} \quad (19)$$

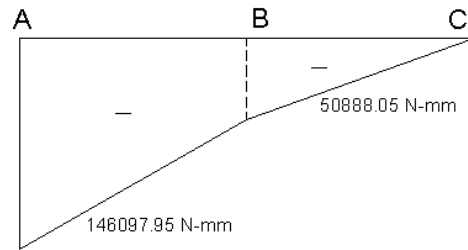


Fig. 18 Bending moment diagram of bottom finger

$$\text{Moment of inertia } (I) = \frac{bd^3}{12} = 87.38 \times 10^3 \text{ mm}^4 \quad (20)$$

$$\text{Section modulus } (Z) = \frac{I}{y} = 5.461 \times 10^3 \text{ mm}^3 \quad (21)$$

$$\text{Stress on finger } (\sigma) = \frac{M}{Z} = 26.75 \text{ MPa} \quad (22)$$

$$\text{Shear stress } (\tau) = \frac{(\text{Max Shear Force}) \times A \times y}{I \times b} = 3.847 \text{ MPa}$$

$$\text{For deflection, } M = EI \frac{d^2y}{dx^2} = -146097.95$$

This gives, Deflection  $y = 0.35 \text{ mm}$

**Stress Analysis of Top Finger:**

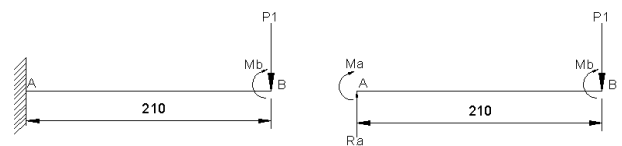


Fig. 19 Free body diagram of top finger

$$\text{Total force, } W_t = [(\text{Component weight} + \text{Finger weight}) \times 9.81] + \text{Gripping force} = W_t = 2626.51 \text{ N} \quad (23)$$

Number of fingers (N) = 2

$$\text{Load on each finger } (P) = \frac{W_t}{N} = 1313.25 \text{ N} \quad (24)$$

$$\text{Therefore, } P_1 = \frac{P}{2} = \frac{1313.25}{2} = 656.625 \text{ N}$$

$$\text{Support reaction at A, } R_a = P_1 = 656.625 \text{ N} \quad (25)$$

$$\text{Moment at A, } M_a = (P_1 \times 210) + M_b = 203553.75 \text{ N-mm}$$

**Shear Force Diagram:**

$$\text{Shear force between (A-B)} = - 656.625 \text{ N} \quad (26)$$

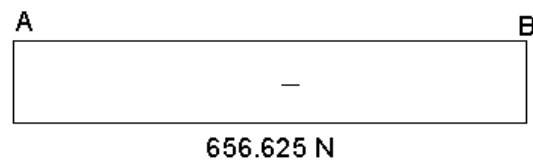


Fig. 20 Shear force diagram

**Bending Moment Diagram:**

Bending Moment at point B = 0

$$\text{Bending Moment at point A} = - (656.625 \times 210) + 65662.5 = - 203553.75 \text{ N-mm} \quad (27)$$

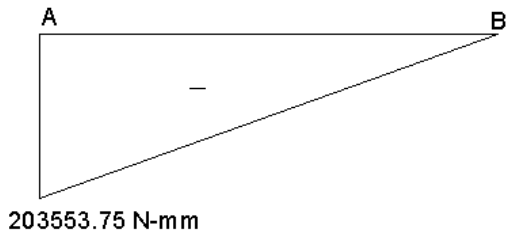


Fig. 21 Bending moment diagram

Stress on finger ( $\sigma$ ) =  $\frac{M}{Z} = 37.27 \text{ MPa}$  (28)

Shear stress ( $\tau$ ) =  $\frac{(\text{Max Shear Force}) \times A \times y}{I \times b} = 3.847 \text{ MPa}$  (29)

For deflection,  $M = EI \frac{d^2y}{dx^2} = -203553.75$  (30)

This gives, Deflection  $y = 0.24 \text{ mm}$

**Analysis considering inertia**

Acceleration (a) =  $\frac{(\text{Maximum velocity})}{(\text{Acceleration time})} = 8 \text{ m/s}^2$  (31)

Force due to inertia ( $F_i$ ) = (Component weight + Finger weight)  $\times a = 698.48 \text{ N}$  (32)

Moment produced due to inertia force ( $M_i$ ) =  $F_i \times 0.35 = 244.47 \text{ N-m}$  (33)

This leads to safe design compared to maximum allowable moment.

Maximum force = [(Component weight + Finger weight)  $\times 9.81$ ] +  $F_i = 1554.99 \text{ N}$  (34)

This leads to safe design compared to maximum allowable force.

**N. EOAT CAD Model**

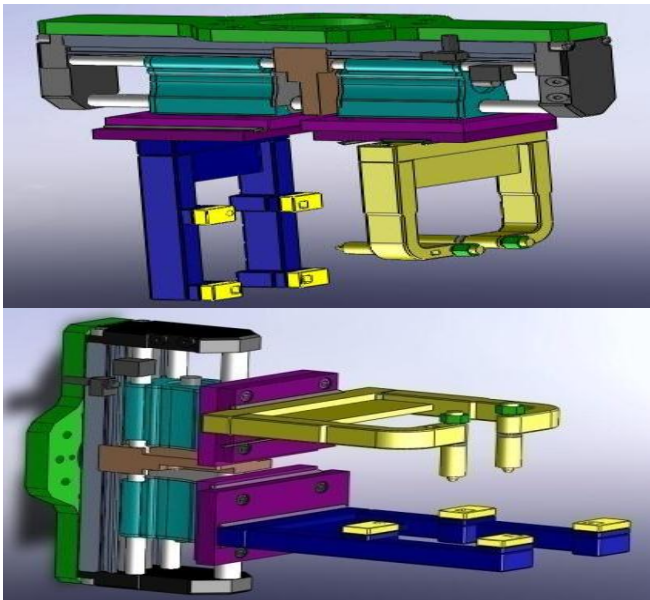


Fig. 22 EOAT CAD model with fingers

**O. Bolted Joint Design**

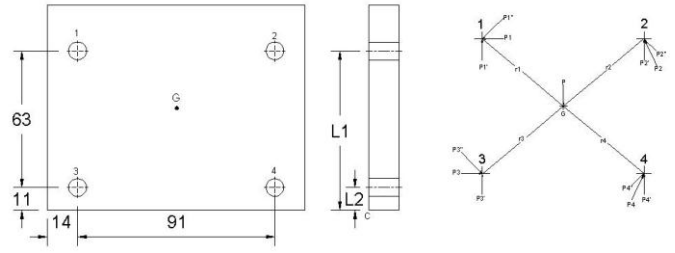


Fig.23. Primary and secondary shear forces

Top and bottom fingers are fastened to the gripper through mounting plates by bolted joint. Bolts of high strength steel are subjected to eccentric loading in shear and eccentric loading perpendicular to axis of bolts.

**Eccentric loading in shear**

**Permissible shear stress**

$\tau = \frac{S_{sy}}{FOS} = \frac{0.55 S_{yt}}{FOS} = 66.367 \text{ N/mm}^2$  (35)

**Primary and secondary shear forces**

$r_1 = r_2 = r_3 = r_4 = r = 79.06 \text{ mm}$  (36)

Primary shear forces with 4 numbers of bolts,

$P1' = P2' = P3' = P4' = \frac{P}{(\text{Number of Bolts})} = 656.63 \text{ N}$

Secondary shear forces,

$P1'' = P2'' = P3'' = P4'' = \frac{(P \times e)}{(4 \times r)} = 2906.90 \text{ N}$  (37)

**Resultant shear force**

$\Theta = 34.70^\circ$

$P1 = \sqrt{(P1'' \cos \Theta - P1')^2 + (P1'' \sin \Theta)^2} = 2396.38 \text{ N}$

$P2 = \sqrt{(P1'' \cos \Theta + P1')^2 + (P1'' \sin \Theta)^2} = 3466.95 \text{ N}$  (38)

**Size of the bolt**

$\tau = \frac{P2}{A}$  (39)

$dc = 8.15 \text{ mm}$

**Eccentric loading perpendicular to axis of bolt**

**Direct shear force in bolt**

$P1' = P2' = P3' = P4' = \frac{P}{(\text{Number of Bolts})} = 656.63 \text{ N}$

Direct shear stress in each bolt is  $\tau = \frac{656.63}{A} \text{ N/mm}^2$  (40)

**Tensile stress in bolt**

$P1'' = \frac{[(Pe) \times L1]}{[2 \times (L1^2 + L2^2)]} = 4289.97 \text{ N}$  (41)

Tensile stress in bolt is  $\sigma = \frac{4289.97}{A} \text{ N/mm}^2$

**Principle stress in bolt**

$\sigma1 = \frac{\sigma t}{2} + \sqrt{(\sigma t/2)^2 + (\tau)^2} = \frac{4388.22}{A}$

Allowable tensile stress in bolt is  $50 \text{ N/mm}^2$

Gives  $A = 88 \text{ mm}^2$

From table of Basic dimensions of ISO metric screw threads, with  $dc = 8.15 \text{ mm}$  and  $A = 88 \text{ mm}^2$ , bolts of M12 are selected.

### III. FEA ANALYSIS

ANSYS 14.5 has been used to do the computational analysis. It is general-purpose finite element analysis software which enables the product development process at less computational and financial expenditure.

#### A. FEA Analysis of Bottom Finger

TABLE I

Boundary conditions for bottom finger

Input	Description
Element type	Brick element
Element size	2 mm and 4 mm
Material	AISI 309S
Young's modules	$210 \times 10^3$ MPa
Poison's ratio	0.29
Forces 1, 2, 3, 4	328.31 N

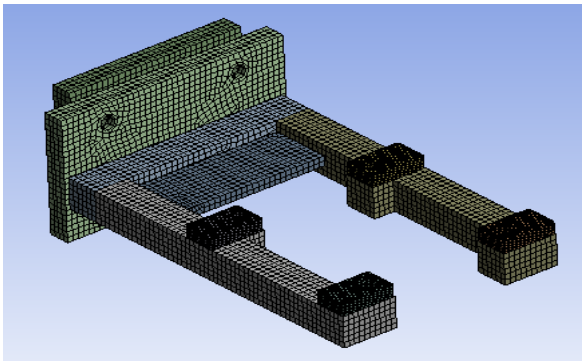


Fig. 24. Meshing of bottom finger

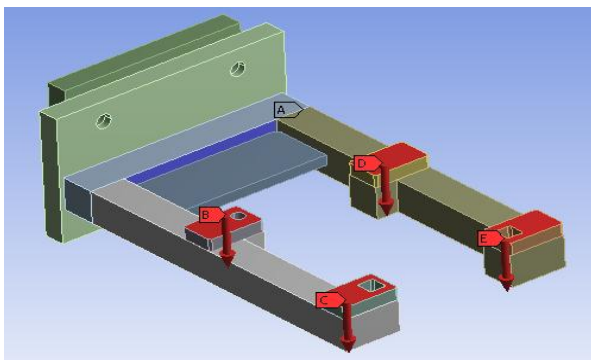


Fig. 25. Boundary conditions of bottom finger

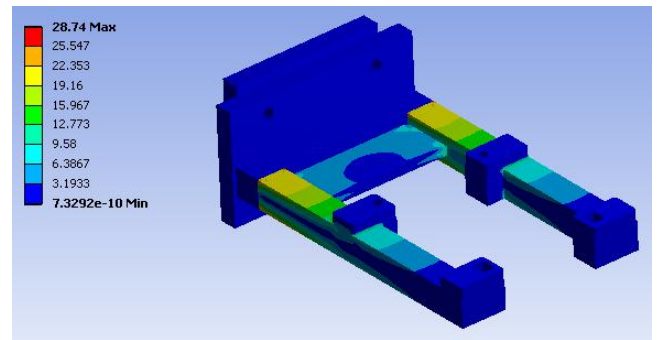


Fig. 26. Stress plot of bottom finger

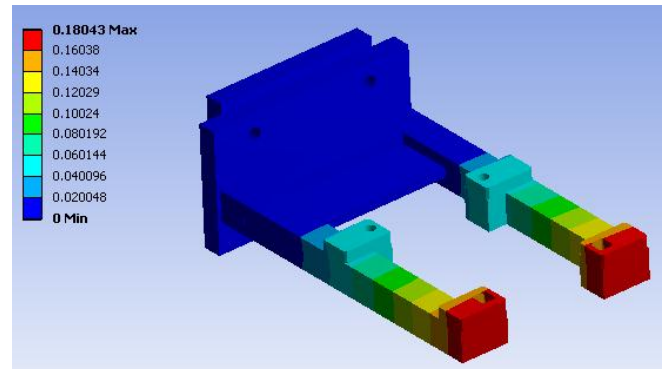


Fig. 27. Deformation plot of bottom finger

From the results of FEA analysis, it can be seen that analytical value of stress for bottom finger is 26.75 MPa and FEA analysis value is 28.74 MPa. Similarly, analytical value of deformation is 0.35 mm and FEA analysis value is 0.18 mm.

#### B. FEA Analysis of Top Finger

TABLE 2

Boundary conditions for top finger

Input	Description
Element type	Brick element
Element size	4 mm
Material	AISI 309S
Young's modules	$210 \times 10^3$ MPa
Poison's ratio	0.29
Forces 1, 2	656.625 N

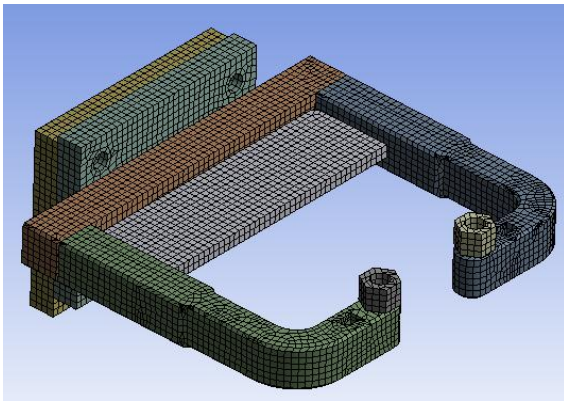


Fig. 28. Meshing of top finger

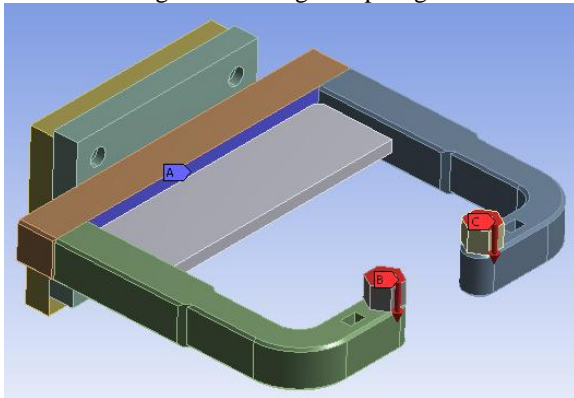


Fig. 29. Boundary conditions of top finger

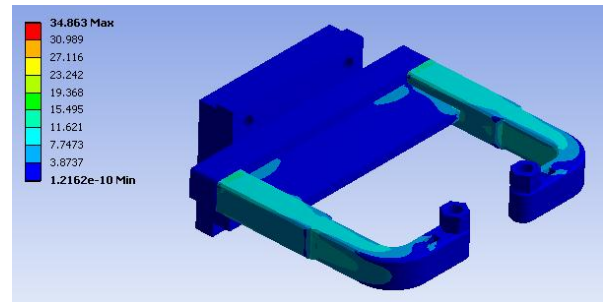


Fig. 30. Stress plot of top finger

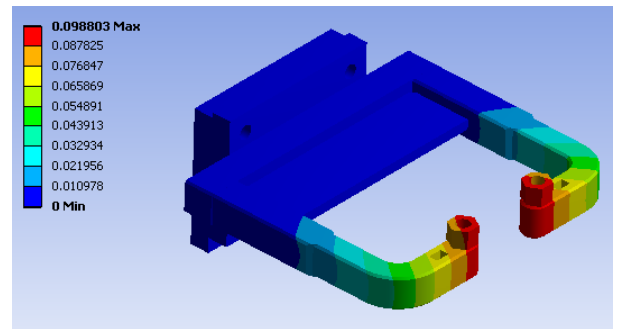


Fig. 31. Deformation of top finger

From the results of FEA analysis, it can be seen that analytical value of stress for top finger is 37.27 MPa and FEA analysis value is 34.86 MPa. Similarly, analytical value of deformation is 0.24 mm and FEA analysis value is 0.098 mm ~ 0.1 mm

**IV. CONCLUSION**

In this work, design of EOAT has been studied. A new kind of EOAT consisting of a pneumatic gripper along with parallel fingers has been analyzed on given conditions. This EOAT can accommodate dimensional variations in components and provides rated flexibility when used in batch production. Flexibility is achieved through compliance unit under change part concept by varying stroke of gripper. This newly design EOAT can withstand pressure variations during washing operations without failure.

TABLE 3  
Result table

No	Quantity	Analytical Value	FEA value
1	Stress on bottom finger ( $\sigma$ )	26.75 MPa	28.74 MPa
2	Deflection in bottom finger ( $\delta$ )	0.35 mm	0.18 mm
3	Stress on top finger ( $\sigma$ )	37.27 MPa	34.86 MPa
4	Deflection in top finger ( $\delta$ )	0.18 mm	0.1 mm

**ACKNOWLEDGMENT**

Thanks to Mr. Rajendra Nisal (MD, Penta Designers and Engineers, Pune), Dr. S.S. Chinchani (HOD, Mechanical Department, VIIT Pune) for their valuable contribution in developing this article.

**NOMENCLATURE**

- F: Gripping force
- FOS: Factor of safety
- L: Tooling length
- M: Moment
- P: Eccentric load
- W: Weight of the component ( $W=mg$ )
- e: Eccentricity
- g: Acceleration due to gravity
- m: Component weight
- n: Number of Fingers
- $\mu$ : Coefficient of static friction
- y: Deflection in finger
- Fa: Total for both jaws
- Mx: Allowable moment, measured from jaw mounting surface
- My: Allowable moment, measured from jaw geometric center
- Mz: Allowable moment, measured from jaw mounting surface

**REFERENCES**

[1] Balkeshwar Singh, N. Sellappan and Kumaradhas, "Evolution of Industrial Robots and their Applications", International Journal of Emerging Technology and Advanced Engineering, Volume 3, Issue 5, pp 763-767, May 2013.

- [2] Mikell. P. Grover, *Industrial Robotics- Technology programming & application*, 2<sup>nd</sup> ed., the University of Michigan, McGraw-Hill, pp 210-290, 1986.
- [3] Samson Khoo Hock Chye, "Design and analysis of robot gripper for 10 kg payload", *Robotics and automation*, pp 1-6, April 2008.
- [4] Burak Dogan, "Development of two fingered and four fingered robotic gripper", *Natural and applied science*, Middle East technical university, pp 7-16, May 2010.
- [5] Yimin Song, Hao Gao, Tao Sun, Gang Dong, Binbin Lian, Yang Qi, "Kinematic analysis and optimal design of a novel 1T3R parallel manipulator with an articulated travelling plate", *Robotics and Computer-Integrated Manufacturing*, pp 508-516, 2014.
- [6] Qiang Zeng, Kornel F. Ehmann, Jian Cao, "Tri-pyramid Robot: Design and kinematic analysis of a 3-DOF translational parallel manipulator", *Robotics and Computer-Integrated Manufacturing*, pp 648-657, 2014.
- [7] Z. Doulgeri, Y. Karayiannidis, "Force position control for a robot finger with a soft tip and kinematic uncertainties", *Robotics and Autonomous Systems*, pp 328-336, 2007.
- [8] Joong-Jo Park, Gab-Soon Kim, "Development of the 6-axis force/moment sensor for an intelligent robot's gripper", *Sensors and Actuators A* 118, pp 127-134, 2005.
- [9] V.C. Moulianitis, N.A. Aspragathos, A.J. Dentsoras, "A model for concept evaluation in design an application to mechatronics design of robot grippers", *Mechatronics* 14, pp 599-622, 2004.
- [10] R. Saravanan, S. Ramabalan, N. Godwin, Raja Ebenezer, C. Dharmaraja, "Evolutionary multi criteria design optimization of robot grippers", *Applied Soft Computing* 9, pp 159-172, 2009.
- [11] Mohammed Khadeeruddin, T.V.S.R.K Prasad, Raffi Mohammed, "Design & Analysis of a Two-jaw parallel Pneumatic Gripper", *International Journal of Computational Engineering Research* Vol. 03, pp 41-46.
- [12] Songhui Nie, Bin Li, Aihong Qiu, Shuguang Gong, "Kinematic configuration analysis of planar mechanisms based on basic kinematic chains", *Mechanism and Machine Theory* 46, pp 1327-1334, 2011.
- [13] Jyh-Jone Lee, Yu-Wei Tsai, "Path synthesis of a finger-type gripping mechanism", *Mechanism and Machine Theory* 40, pp 1209-1223, 2005.
- [14] Dalibor Petkovic, Shahaboddin Shamshirband, Javed Iqbal, Nor Badrul Anuar, Nenad D. Pavlovic, Miss Laiha Mat Kiah, "Adaptive neuro-fuzzy prediction of grasping object weight for passively compliant gripper", *Applied soft computing* 22, pp 424-431, 2014.
- [15] Rim Boughdiri, Habib Nasser, Hala Bezine, Nacer K. M'Sirdi, Adel M. Alimi, Aziz Naamane, "Dynamic Modeling and Control of a Multi-Fingered Robot Hand for Grasping Task", *International Symposium on Robotics and Intelligent Sensors*, *Procedia Engineering* 41, pp 923-931, 2012.
- [16] Sandeep Krishnan, Laxman Saggere, "Design and development of a novel micro-clasp gripper for micromanipulation of complex-shaped objects", *Sensors and actuators A: Physics* 176, pp 110-123, 2012.
- [17] Arockia Selvakumar A, Arul Kumar M, "Experimental investigation on position analysis of 3 DOF parallel manipulators", *12th global congress on manufacturing and management*, pp 1126-1134, 2014.
- [18] Gualtiero Fantoni, Saverio Capiferri, Jacopo Tilli, "Method for supporting the selection of robot grippers", *24<sup>th</sup> CIRP design conference* pp 330-335, 2014.
- [19] Alaa Hassana, Mouhammad Abomoharam, "Design of a single DOF gripper based on four-bar and slider-crank mechanism for educational purposes", *24<sup>th</sup> CIRP design conference*, pp 379-384, 2014.
- [20] Yi Lu, Peng Wang, Zhuolei Hou, Bo Hu, Chunping Su, Jianda Han, "Kinetostatic analysis of a novel 6-DoF 3UPS parallel manipulator with multi-fingers", *Mechanism and Machine Theory* 78, pp 36-50, 2014.
- [21] Nobuaki Nakazawa, Il-hwan Kim, Hikaru Inooka, Ryojun Ikeura, "Force control of a robot gripper based on human grasping schemes", *Control Engineering Practice* 9, pp 735-742, 2001.
- [22] Olivier Millet, Paul Bernardoni, Stéphane Régnier, Philippe Bidaud, "Electrostatic actuated micro gripper using an amplification mechanism", *Sensors and Actuators*, pp 371-378, 2004.

